Comparative study of gamma ray shielding competence of WO 3 -TeO 2 -PbO glass system to different glasses and concretes

Article *in* Materials Chemistry and Physics · April 2018
DOI: 10.1016/j.matchemphys.2018.04.019

CITATION
1

READS
190

8 authors, including:

Dhammajyot K Gaikwad
Dr. Babasaheb Ambedkar Marathwada University
20 PUBLICATIONS **41** CITATIONS
SEE PROFILE

Shamsan Obaid
Dr. Babasaheb Ambedkar Marathwada University
9 PUBLICATIONS **13** CITATIONS
SEE PROFILE

M. I. Sayyed
University of Tabuk
68 PUBLICATIONS **536** CITATIONS
SEE PROFILE

R R Bhosale
Dr. Babasaheb Ambedkar Marathwada University
13 PUBLICATIONS **11** CITATIONS
SEE PROFILE

Materials Chemistry and Physics 213 (2018) 508–517

Contents lists available at ScienceDirect

Materials Chemistry and Physics

journal homepage: www.elsevier.com/locate/matchemphys

Comparative study of gamma ray shielding competence of WO_3-TeO_2-PbO glass system to different glasses and concretes

D.K. Gaikwad [a, *], Shamsan S. Obaid [a], M.I. Sayyed [b], R.R. Bhosale [a], V.V. Awasarmol [a], Ashok Kumar [c], M.D. Shirsat [a, d], P.P. Pawar [a]

[a] Department of Physics, Dr. Babasaheb Ambedkar Marathwada University, Aurangabad, 431004, India
[b] Physics Department, University of Tabuk, Tabuk, Saudi Arabia
[c] Department of Physics, University College, Benra-Dhuri, Punjab, India
[d] RUSA Center for Advance Center Technology, Dr. Babasaheb Ambedkar Marathwada University, Aurangabad, 431004, India

HIGHLIGHTS

- Present work explores the gamma ray shielding properties of WO_3-TeO_2-PbO glasses.
- Mass attenuation coefficients, half value layers and mean free paths have been determined to check shielding effectiveness.
- Exposure buildup factor has also been studied at different penetration depth.
- WO3-TeO2-PbO glasses are compared with standard shielding concretes and glasses.

ARTICLE INFO

Article history:
Received 4 January 2018
Received in revised form
28 March 2018
Accepted 5 April 2018
Available online 14 April 2018

Keywords:
Shielding
Glass
Mass attenuation coefficient
G-P fitting method

ABSTRACT

The photon attenuation coefficients of $20WO_3$-(80-x) TeO_2-xPbO (where x = 10, 12.5, 15, 17.5 and 20 mol %) tellurite glasses have been studied in the energy region of 1 keV–100 GeV. The addition of PbO into the glass system increases the mass attenuation coefficients and decreases the mean free path and the half value layer. Moreover, WTP5 which contains 20 mol% of PbO shows the highest radiation shielding capability. In addition, tellurite glasses have been compared with other glass systems, some standard shielding concretes and three commercial window glasses in terms of mass attenuation coefficients, mean free path and half value layer. The G-P fitting method also used to evaluate the exposure buildup factor of the present glasses. The exposure buildup factor of the present samples has also been compared with the other glasses, lead and concretes. It has-been found that the glasses under study have higher values of mass attenuation coefficients than that of commercial window glasses. Also, it has been found that the present glasses have lower mean free path, thus possess better shielding properties than different concrete samples and other selected glasses.

1. Introduction

With the advances of technology, the use of radioactive sources has been increased tremendously for wide applications in the nuclear reactor, medical diagnostics, medicine, agriculture, petrochemical, nuclear industries, manufacture, accelerator technology, space research, etc. Exposure to highly penetrating nuclear radiation emitted from radioactive sources is harmful to humans, animals and plants. Thus, the fabrication and design new effective radiation shielding materials are essential in order to avoid the deleterious effects of nuclear radiation on human health. Recently, the invention of a variety of shielding materials has gained great attention among the research community to address shielding of hazardous radiations. Concretes are the most widely used shielding materials in nuclear reactors, accelerators and radiology hospitals construction [1]. Concrete is popular in radiation shielding design due to its abundance, availability, affordability, durability, and acceptable radiation shielding competence [2]. Though crack formation, leaching, water content gets evaporates due to exposure of high energy radiation results in the porous formation, decrease in density and structural strength are the associated shortcomings of

* Corresponding author.
E-mail addresses: dhammajyotg26@gmail.com, physics.dkg@bamu.ac.in (D.K. Gaikwad).

https://doi.org/10.1016/j.matchemphys.2018.04.019
0254-0584/

concretes as shielding materials [3]. High attenuation of radiation, negligible irradiation effects on structural and mechanical properties of the material, homogeneous of density and composition are the essential properties of radiation shielding design [4,5]. Glasses are the attractive candidates in this context, as glasses absorbed gamma rays and neutrons to a great extent compared to concretes [5,6]. Additionally, they provide transparency to visible light while absorbing ionizing radiation, excellent homogeneity, and range of additive oxides which can be helpful to alter the density, mechanical and physical properties of glasses [6,7].

Among the glasses, tellurite glasses show substantial importance for both basic science and engineering technology research due to low melting temperature, high electrical conductivity, high thermal stability and density, good mechanical strength and chemical durability, low melting and verification temperatures, high dielectric constant, excellent moisture and corrosion resistance, etc. [7,8]. However, Tellurium oxide (TeO_2) is a well-known conditional glass former which needs an additional modifier to form glass under normal quenching condition [9]. The modification of glass forming ability and improvement in optical, thermal and mechanical properties can be achieved by introducing heavy metal oxides (such as PbO, Bi_2O_3, MoO_3, WO_3andNb_2O_5) into tellurium oxide glasses [10,11]. Lead oxide (PbO) plays an influential role in glass formation as it acts as network modifier and network former [12]. PbO, $Bi_2O_3$and WO_3 contained glasses are the promising materials for waste storage and infrared transmission applications [13]. Heavy metal oxides based glasses are the potent radiation shielding materials as they provide a large attenuation cross section and a rate of degrading their optical and mechanical properties due to high energy photons is very small [14].

To design effective shielding materials for the particle accelerator, nuclear facilities, laboratories, radiation therapy facilities and other civil constructions, materials should be tested first by studying various shielding parameters and other available simulation tools. The mass attenuation coefficient (μ/ρ), mean free path (MFP), half value layer (HVL) and exposure buildup factor (EBF) are required quantities to evaluate shielding effectiveness of any materials (alloys, glass, concrete, etc) [6]. The intensity of a monochromatic narrow beam of photons attenuated by thin absorber follows Lambert's Beer law. If this law doesn't hold due to a failure of any condition, buildup factor is being used to make Lamberts Beer Law [15] valid. The EBF is most widely used to design shielding materials for radiation sites (nuclear reactor, accelerators, medical facilities, etc.) [15]. Extensive investigation on the attenuation coefficients of glasses [16,17,18,19], concretes [20,21,22], rocks [23,24], alloys [25,26], organic compounds [27,28,29,30] and other materials [31,32] have reported for their medical and radiation protection applications. The Buildup factor is important to choose the appropriate thickness or control the thickness of glasses and concretes for radiation shield [33,34]. Sayyed [35] has been investigated the shielding parameters in the TeO_2-B_2O_3-Bi_2O_3-ZnO quaternary tellurium glasses. He compared the results with the standard shielding materials and showed that the tellurium glasses may be useful for the development of efficient gamma-ray shielding materials. Mostafa et al. [36] have been studied WO_3 doped PbO-B_2O_3-P_2O_5 glass system and reported that the gamma ray absorption capability increases with the WO_3 content in the glass matrix.

In the present investigation, heavy metal oxides base ternary WO_3-TeO_2-PbO glasses have been studied for radiation application. The aim of the present work is (a) to explore the gamma ray shielding properties of ternary heavy metal oxides tellurite glasses by calculating shielding parameters such as μ/ρ and EBF (b) comparison of the present glass samples with different glass systems, some standard shielding concretes and three commercial window glasses to seek the availability of utilizing the WO_3-TeO_2-PbO glasses with respect to gamma rayprotection.

2. Materials and computational method

In the present work, 20WO_3-(80-x) TeO_2-xPbO (where x = 10, 12.5, 15, 17.5 and 20mol %) tellurite glasses have been selected as shown in Table 1 [37]. For the purpose of comparison, some shielding materials from the literature have been chosen as follows; type A, type B and type C window glasses [38]; normal weight concretes (Silicates, Limestone and silicates, Portland, Rocky flats and limestone) [39]; 40PbO-10BaO-50B_2O_3 [40]; 50Bi_2O_3-30B_2O_3-5TeO_2-15SiO_2 [41]; 40Bi_2O_3-10BaO-50P_2O_5 [3]; 50PbO-50B_2O_3 and 50Bi_2O_3-50B_2O_3 [42]; G6 [43] and S7 [44] glasses; Bismuth borosilicate glass 20% (BS) [45]; Lead [46]; Ordinary (OC), Ilmenite–limonite (IL), Steel-scrap (SC), Steel-magnetite (SM) [47] concretes; 10WO_3-40MoO_3-50TeO_2 (50Te); 10WO_3-20MoO_3-70TeO_2 (70Te) and 10WO_3-10MoO_3-80TeO_2 (80Te) glasses [48].

2.1. Half value layer and mean free path

The mass attenuation coefficients (μ/ρ) of an absorbing media constituent of different elementscan are determined by mixture rule given by following equation [49];

$$\frac{\mu}{\rho} = \sum_i W_i \left(\frac{\mu}{\rho}\right)_i \quad (1)$$

Where W_i is fraction by weight of ith elements. The $(\mu/\rho)_i$ values of the (O, Te, W and Pb) elements in the energy range 1 keV–100 GeV have been taken from XCOM program [50].

Mean free path (MFP) is the average distance between two successive interactions, while the thickness of an absorber that reduces the intensity of incident photon by half of its initial value is known as half value layer, which can be calculated using Eqs. (2) and (3) respectively [6,7]:

$$MFP = \frac{1}{\mu} \quad (2)$$

$$HVL = \frac{\ln(2)}{\mu} = \frac{0.693}{\mu} \quad (3)$$

where μ is the linear attenuation coefficient.

2.2. Exposure buildup factor (EBF)

The exposure buildup factor (EBF) of the selected glass samples has been computed by utilizing G-P fitting parameters b, c, a, X_k and d [46]. Computation of EBF has been done in three steps. These steps include the (1) calculation of the equivalent atomic number (Z_{eq}) followed by (2) computation of G-P fitting parameters and finally (3) calculation of EBF values.

The equivalent atomic number, Z_{eq} is a single quantity utilized to characterize the WO_3TeO_2-PbO glass samples properties in terms of

Table 1
Chemical composition and density of 20WO_3-(80-x)TeO_2-xPbO glasses.

Sample Code	x	Mole fraction of constituent oxides	Density (g/cm^3)
WTP1	10	WO_3(0.2), TeO_2 (0.7), PbO(0.1)	5.5875
WTP2	12.5	WO_3 (0.2), TeO_2(0.675), PbO(0.125)	5.7179
WTP3	15	WO_3(0.2), TeO_2(0.65), PbO(0.15)	5.7379
WTP4	17.5	WO_3(0.2), TeO_2(0.625), PbO(0.175)	5.8851
WTP5	20	WO_3(0.2), TeO_2(0.6), PbO(0.2)	5.9012

equivalent elements. For the present glass samples, Z_{eq} can be calculated from the ratio of the Compton partial mass attenuation coefficient (i.e. $(\mu/\rho)_{Compton}$) to the total mass attenuation coefficient (i.e. $(\mu/\rho)_{Total}$) at certain energy, with the help of the following equation [51,52]:

$$Z_{eq} = \frac{Z_1(logR_2 - logR) + Z_2(logR - \log R_1)}{logR_2 - logR_1} \quad (4)$$

where Z_1 and Z_2 represent the atomic numbers of elements corresponding to the ratios R_1 and R_2 respectively and R is the ratio $((\mu/\rho)_{Compton}/(\mu/\rho)_{Total})$ for the glass samples at a certain energy. For example the ratio $R = (\mu/\rho)_{Compton}/(\mu/\rho)_{total}$ of WTP1 glass sample 0.1 MeV is 0.0526, which lies between $R_1 = 0.0539$ of $Z_1 = 55$ and $R_2 = 0.0513$ of $Z_2 = 56$, using Eq. (4) the $Z_{eq} = 55.51$. The obtained Z_{eq} for the present glass samples then used to calculate the five G-P fitting parameters (a, b, c, d and X_k) using the following relation [15]:

$$a = \frac{a_1(logZ_2 - logZ_{eq}) + a_2(logZ_{eq} - logZ_1)}{logZ_2 - logZ_1} \quad (5)$$

where a_1 and a_2 are the G-P fitting parameters corresponding to the Z_1 and Z_2 respectively at a given energy.

From the five G-P fitting parameters we can evaluate the EBF values for the selected glasses using following equation [53].

$$B(E, X) = 1 + \frac{b-1}{K-1}(K^x - 1) \quad for\ K \neq 1 \quad (6)$$

$$B(K, X) = 1 + (b-1)x \quad for\ K = 1 \quad (7)$$

where,

$$K(E, x) = cx^a + d\frac{tanh\left(\frac{x}{X_k} - 2\right) - tanh(-2)}{1 - \tanh(-2)} \quad for\ x \leq 40\ mfp \quad (8)$$

where E and x are incident photon energy and the penetration depth respectively.

3. Results and discussion

The mass attenuation coefficients of $20WO_3$-(80-x) TeO_2-xPbO glasses (where x = 10, 12.5, 15, 17.5 and 20 mol %) have been computed with XCOM in an energy range of 1 keV–100 GeV. The variations of μ/ρ with incident photon energies have been shown in Fig. 1(a). On the basis of the relative dominance of the three photon interaction mechanisms (i.e. Photoelectric absorption, Compton scattering and pair production), the considerable changes in μ/ρ were observed. It is noticed that in the low energy region (1 keV–0.4 MeV); the variation in is μ/ρ the same for all samples. The μ/ρ values of the present glasses are very large in this low photon energy region (in order of 7×10^3 cm^2/g) and then decrease sharply with energy. It is due to the dominance of the photoelectric effect in the low energy region. The cross section of photoelectric effect changes with the atomic number as Z^{4-5} and changes with the energy of the photon as $1/E^{3.5}$. Hence, we found that the glass samples have highest μ/ρ values in the low energy region where the photoelectric effect predominates, and the μ/ρ values decrease as the energy of photon increases.

The sharp discontinuities in the values of μ/ρ are observed at different energies shown in Table 2. It is due to the fact that K, L and M-absorption edges of elements Te, W and Pb present in these samples lies at these energies. In the medium energy region (0.4 MeV–6 MeV) the values of μ/ρ are nearly same for all the samples. Thus μ/ρ is independent of chemical composition in the medium energy region, which is due to the dominance of the Compton scattering process. Due to the inverse variation of the Compton scattering cross-section with energy; the μ/ρ values are found to decrease in the medium energy region. In the high energy region (above 6 MeV) chemical composition and energy both effects μ/ρ. In this high energy region, the pair production process is the dominant interaction process, and it is known that the cross section of pair production is directly proportional to Z^2, therefore, we can observe that the μ/ρ values slowly increase in this energy region.

Additionally, Fig. 1(a) revealed that the μ/ρ values increase with the addition of PbO. This increase in μ/ρ values can be attributed to the replacement of a lighter molecule (TeO_2) by a heavier one (PbO). Therefore, we can observe from Fig. 1 that the μ/ρ values possess maxima for WTP5 (which contains 20% PbO) and minima for WTP1 in the high energy region. It is due to the presence of high concentration of PbO in WTP5 sample. Hence, we can conclude that WTP5 glass sample has superior shielding properties among the present samples.

The μ/ρ values of $20WO_3$-(80-x)TeO_2-xPbO glasses were compared with the experimental μ/ρ values of $10WO_3$-$40MoO_3$-$50TeO_2$ (50Te); $10WO_3$-$20MoO_3$-$70TeO_2$ (70Te) and $10WO_3$-$10MoO_3$-$80TeO_2$ (80Te) glasses [48] at 276.4 keV, 302.8 keV, 356 keV and 383.8 keV as shown in Fig. 1(b). It is clear from the Figure that the $20WO_3$-(80-x) TeO2-xPbO glasses have higher μ/ρ values than 50Te, 70Te and 80Te glasses. Thus, we can conclude that the $20WO_3$-(80-x) TeO2-xPbO glasses possess better shielding capabilities than 50Te, 70Te and 80Te glasses. Additionally, the comparison of the μ/ρ values of the $20WO_3$-(80-x) TeO2-xPbO glasses with commercial glasses have been shown in Fig. 2. It is found that present glasses possess higher μ/ρ values compared to the commercial glasses for all energies except for the energy region where the Compton scattering process is dominant. But in the medium energy region, μ/ρ for the present samples and commercial glasses are nearly same. It is due to that μ/ρ is independent of the chemical composition of Compton scattering dominant region.

The variation of MFP of $20WO_3$-(80-x)TeO_2-xPbO glasses with energy is shown in Fig. 3 in the energy region 1 keV to 100 GeV for the total interaction process. MFP of the present samples shows an increasing trend up to 6 MeV. MFP values are very low of the order of (10^{-6}-10^{-2}) cm up to 100 keV, but have increasing behavior in this energy region as it is shown in Fig. 3. For 100 keV to 6 MeV; MFP values increase sharply and possess maxima at 6 MeV. Thereafter, MFP values decrease sharply up to 100 MeV and thereafter above 100 MeV; MFP decreases moderately. The

Table 2
Photon energies (keV) of absorption edges for elements present in $20WO_3$-(80-x)TeO_2-xPbO glasses.

Element	Z	M5	M4	M3	M2	M1	L3	L2	L1	K
Te	52	–	–	–	–	1.006	4.341	4.612	4.939	31.810
W	74	1.809	1.872	2.281	2.575	2.820	10.210	11.540	12.100	69.530
Pb	82	2.484	2.586	3.066	3.554	3.851	13.040	15.200	15.860	88.000

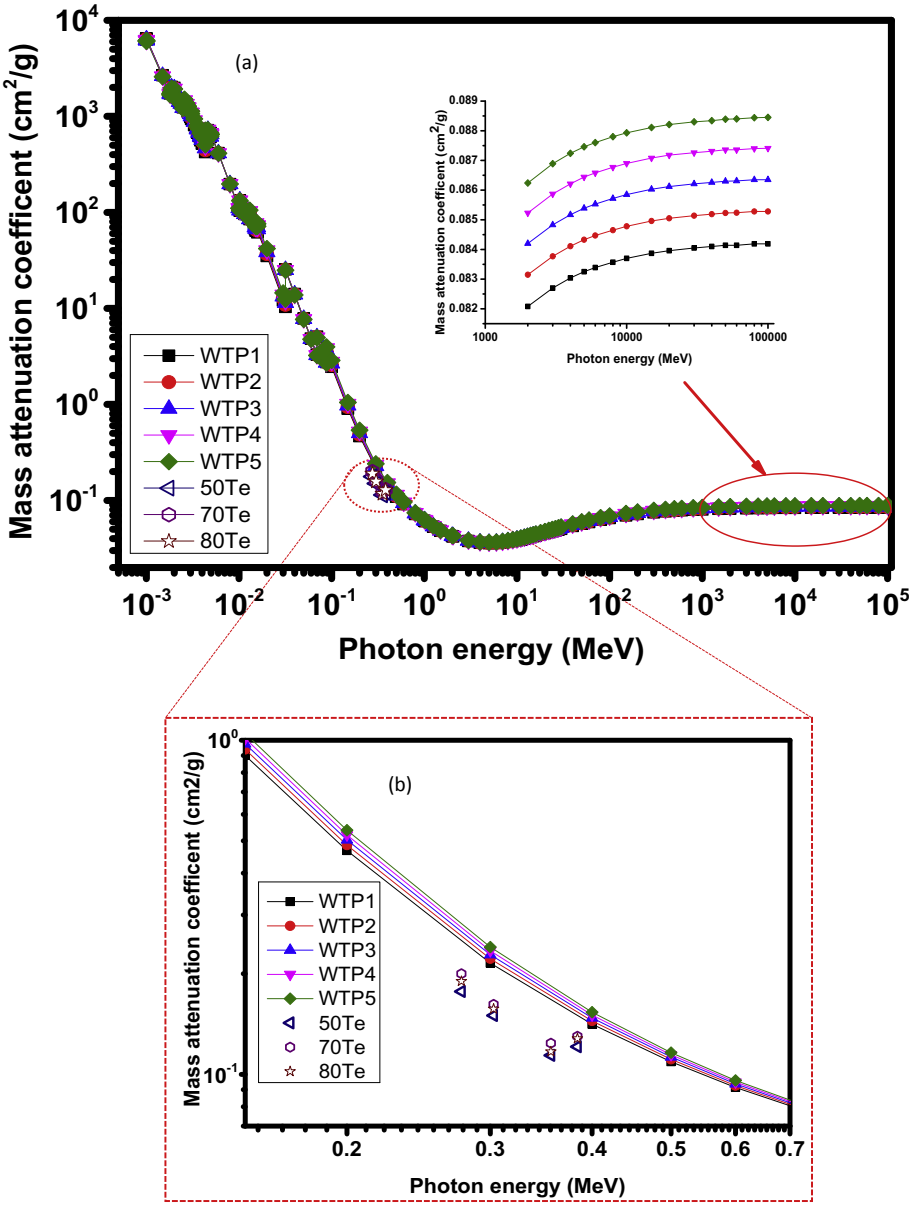

Fig. 1. Total mass attenuation coefficients of $20WO_3$-(80-x)TeO_2-xPbO glasses with photon energy in the energy range 1 keV–100 GeV.

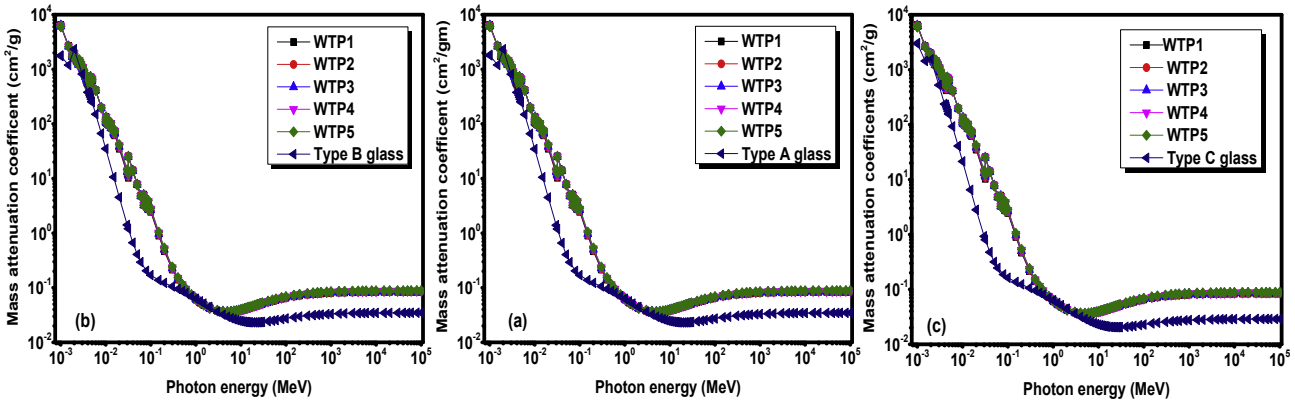

Fig. 2. Mass attenuation coefficents of $20WO_3$-(80-x)TeO_2-xPbO glasses with commercial window glasses.

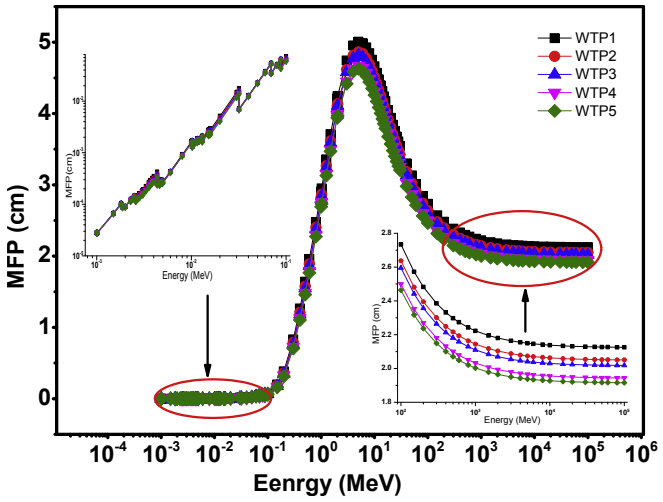

Fig. 3. MFP of $20WO_3$-(80-x)TeO_2-xPbO glasses with energy in the energy range 1 keV–100 GeV.

variation for MFP with incident photon energy can be explained by the three photon interaction mechanisms similar to above μ/ρ. From Fig. 3 one can see that when PbO concentration increases, the MFP values are decreasing. It is due to the increase in the density value with increasing PbO concentration. It is known that the MFP for any glass sample is inversely proportional to the density of the glass sample, and according to Table 1, the addition of PbO leads to an increase in the density of the present glasses, thus the MFP values decrease. Therefore, we can see that the MFP of WTP5 (which has the maximum PbO content and the highest density) is lower than other glasses. Thus WTP5 possesses best shielding competence among the selected samples.

MFP and HVL are very important parameters in deciding the radiation shielding efficiency of a material. The comparison of MFP $20WO_3$-(80-x)TeO_2-xPbO glasses with normal weight concretes have been represented in Fig. 4 in the energy range of 1 keV to 100 GeV. For this comparison, we have selected silicates, limestones and silicates, portland, rocky flats, lime stone and type 04 as normal weight concretes. MFP of the selected glasses is nearly same as MFP of the selected normal weight concretes in the energy range 1 keV–50 keV. Thus, the gamma ray shielding efficiency of the selected glasses is nearly same as that of the normal weight concretes up to 50 keV. From 50 keV to 100 GeV; the MFP of the present glasses are lower than the MFP of the normal weight concretes. Thus, the present glass samples possess the better shielding competence to the normal weight concretes in this wide energy region above 50 keV. It is due to the presence of heavy metal oxides of WO_3, $TeO_2$and PbO present in the glass samples.

The HVL of the $20WO_3$-(80-x)TeO_2-xPbO glasses have been compared with 40PbO.10BaO.$50B_2O_3$; $40Bi_2O_3$.10BaO.$50P_2O_5$; $50Bi_2O_3$.$30B_2O_3$.$5TeO_2$.$15SiO_2$; 50PbO.$50B_2O_3$; 40PbO.10-Bi_2O_3.$49.5B_2O_3$.0.5FeO and $50Bi_2O_3$.$50B_2O_3$ glasses in the energy range of 1 keV to 100 GeV and the results are presented in Fig. 5. The HVL of the present glasses is nearly same as 40PbO.10-BaO.$50B_2O_3$; $40Bi_2O_3$.10BaO.$50P_2O_5$; $50Bi_2O_3$.$30B_2O_3$.$5TeO_2$.$15SiO_2$ and $50Bi_2O_3$.$50B_2O_3$up to 3 MeV. Beyond 3 MeV, HVL of the present glasses is nearly half than that of the mentioned above glasses. Thus, the present glasses are equally effective as

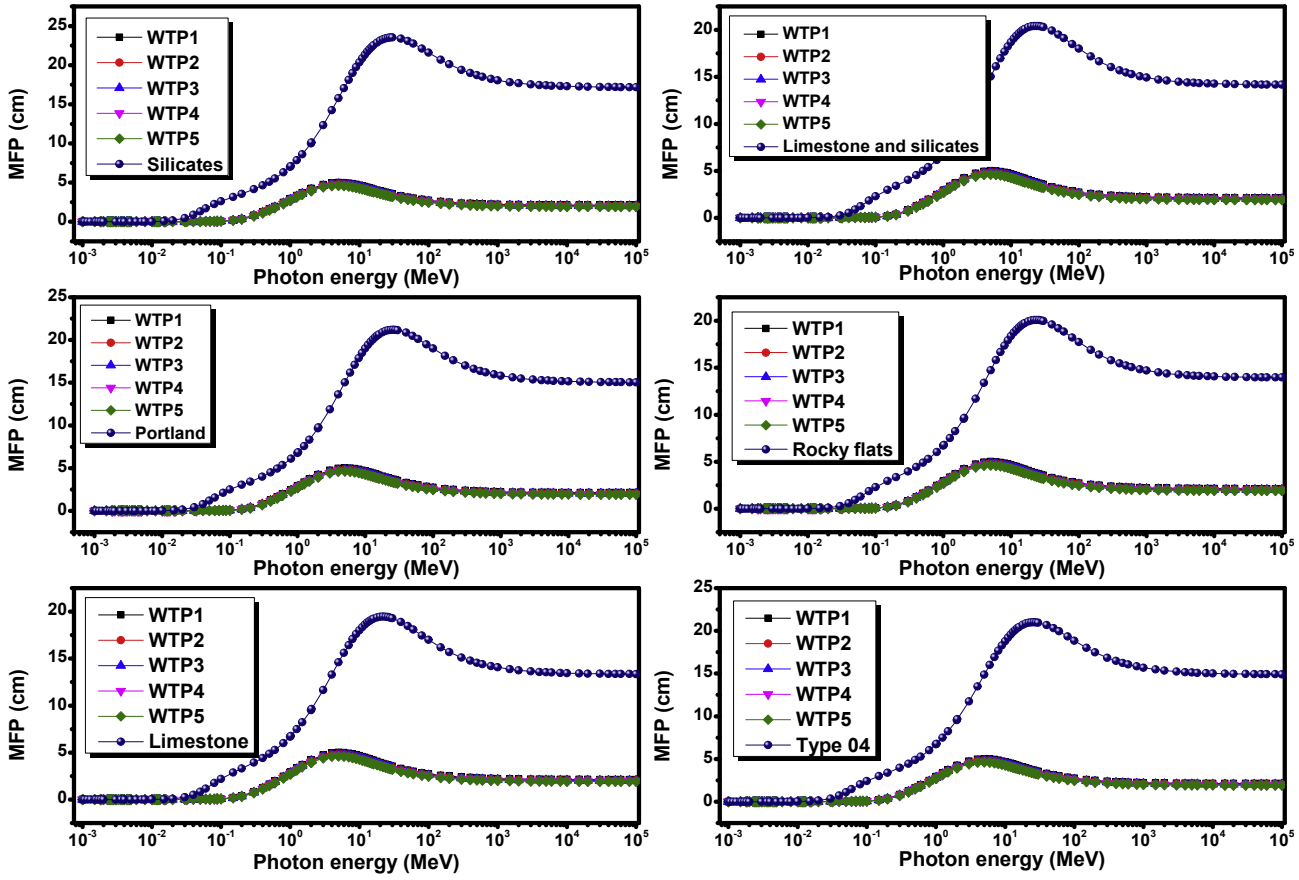

Fig. 4. Comparison of MFP of $20WO_3$-(80-x)TeO_2-xPbO glasses with normal weight concretes.

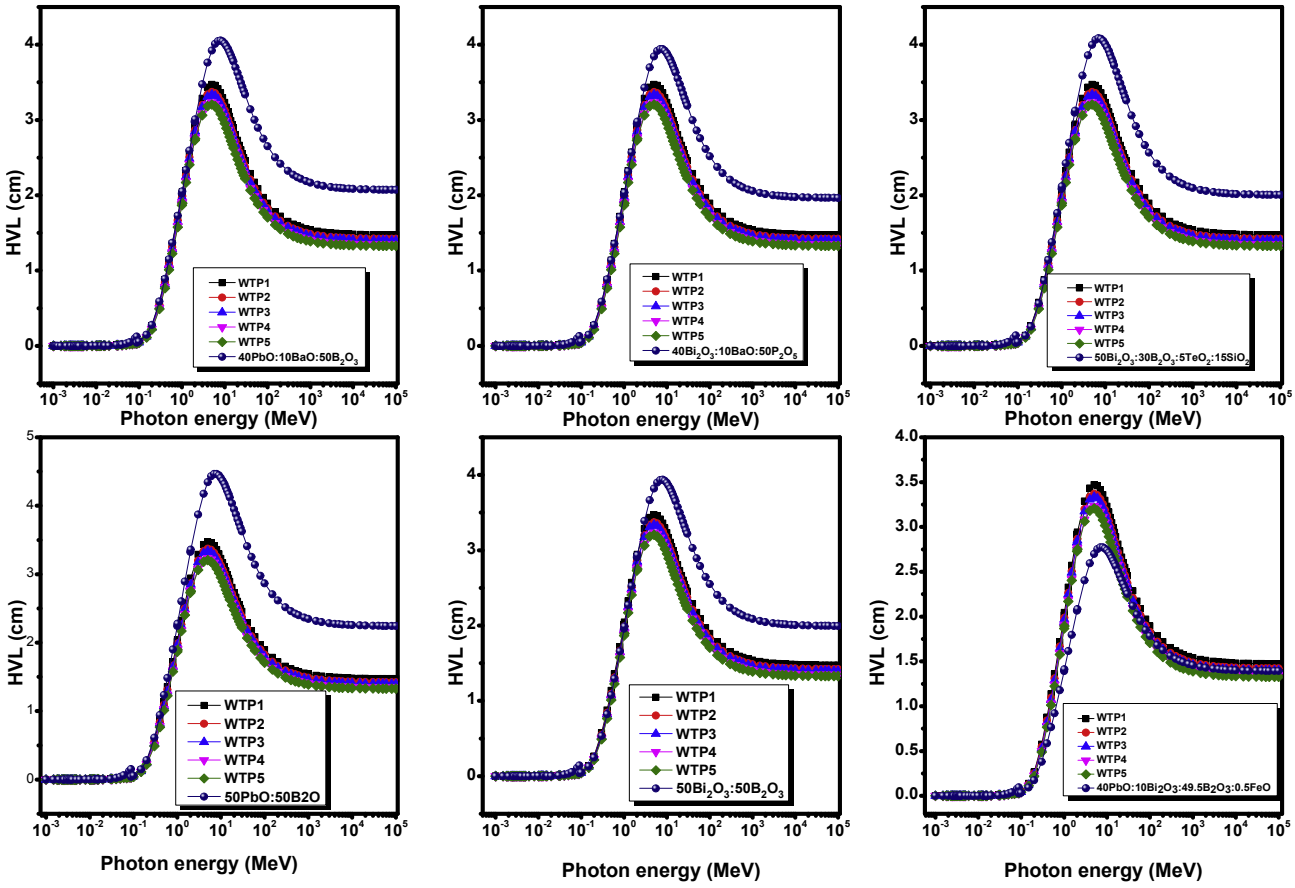

Fig. 5. Comparison of MFP of $20WO_3$-(80-x)TeO_2-xPbO glasses with different shielding glasses.

Table 3
Equivalent atomic number of $20WO_3$-(80-x)TeO_2-xPbO glasses.

Energy (MeV)	Equivalent atomic number (Z_{eq})				
	WTP1	WTP2	WTP3	WTP4	WTP5
0.015	28.422	28.706	28.982	29.259	29.584
0.020	29.629	30.162	30.713	31.248	31.773
0.030	30.065	30.609	31.155	31.684	32.202
0.040	44.314	44.290	44.252	44.228	44.185
0.050	44.677	44.628	44.591	44.556	44.504
0.060	44.925	44.878	44.844	44.793	44.744
0.080	51.321	51.310	51.292	51.265	51.247
0.100	55.510	56.373	57.221	58.068	58.886
0.150	56.305	57.194	58.092	58.940	59.811
0.200	56.743	57.666	58.701	59.437	60.296
0.300	57.305	58.240	59.152	60.049	60.911
0.400	57.624	58.593	59.517	60.417	61.274
0.500	57.862	58.816	59.738	60.662	61.514
0.600	57.977	58.959	59.885	60.800	61.681
0.800	58.131	59.125	60.070	60.991	61.863
1.000	58.196	59.185	60.159	61.064	61.947
1.500	57.947	58.425	59.357	60.319	61.184
2.000	55.286	56.221	57.256	58.163	59.066
3.000	51.568	52.527	53.464	54.360	55.225
4.000	49.724	50.657	51.490	52.332	53.282
5.000	48.690	49.560	50.404	51.250	52.074
6.000	48.094	48.914	49.749	50.526	51.356
8.000	47.377	48.149	48.931	49.700	50.503
10.000	46.996	47.715	48.485	49.264	50.064
15.000	46.657	47.403	48.139	48.895	49.644

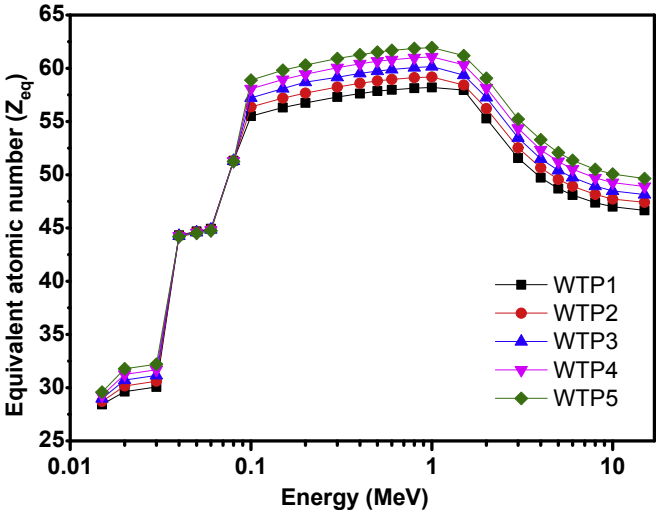

Fig. 6. Z_{eq} of $20WO_3$-(80-x)TeO_2-xPbO glasses.

Table 4
Exposure G-P fitting parameters of WTP1glass sample.

Energy (MeV)	WTP1				
	b	c	A	X_k	D
0.015	1.003	1.767	−0.450	7.966	0.310
0.020	1.988	1.320	0.295	12.374	−0.398
0.030	1.192	0.407	0.199	13.320	−0.062
0.040	3.825	0.606	0.091	24.303	−0.062
0.050	3.366	0.346	0.089	15.248	−0.143
0.060	2.905	0.217	0.056	5.927	−0.063
0.080	1.886	0.080	0.508	15.751	−0.125
0.100	1.545	0.143	0.319	16.956	−0.050
0.150	1.211	0.298	0.304	13.886	−0.171
0.200	1.211	0.463	0.189	14.307	−0.101
0.300	1.285	0.569	0.135	13.831	−0.063
0.400	1.356	0.685	0.095	14.189	−0.052
0.500	1.407	0.752	0.074	14.143	−0.044
0.600	1.444	0.802	0.058	14.631	−0.036
0.800	1.577	0.926	0.025	13.664	−0.024
1.000	1.587	0.965	0.016	13.295	−0.022
1.500	1.497	1.026	0.002	13.991	−0.017
2.000	1.555	1.090	−0.011	13.094	−0.013
3.000	1.534	1.030	0.013	13.218	−0.040
4.000	1.480	1.032	0.016	13.411	−0.044
5.000	1.499	0.952	0.046	13.659	−0.072
6.000	1.495	0.922	0.057	13.830	−0.080
8.000	1.529	0.891	0.078	14.154	−0.098
10.000	1.504	1.033	0.048	14.180	−0.071
15.000	1.586	1.177	0.029	13.995	−0.058

Table 5
Exposure G-P fitting parameters of WTP2glass sample.

Energy (MeV)	WTP2				
	b	c	A	X_k	D
0.015	1.002	1.904	−0.381	9.537	0.281
0.020	1.263	0.418	0.643	11.193	−0.889
0.030	2.627	0.808	0.146	24.343	−0.153
0.040	3.834	0.585	0.091	24.233	−0.059
0.050	3.348	0.324	0.060	15.014	−0.129
0.060	2.880	0.206	0.109	6.512	−0.067
0.080	1.883	0.078	0.519	15.740	−0.084
0.100	1.424	0.050	0.678	14.042	−0.264
0.150	1.195	0.219	0.383	13.758	−0.261
0.200	1.171	0.409	0.218	14.187	−0.116
0.300	1.290	0.571	0.134	13.833	−0.063
0.400	1.359	0.687	0.094	14.185	−0.052
0.500	1.411	0.755	0.073	14.141	−0.044
0.600	1.446	0.803	0.072	13.752	−0.036
0.800	1.578	0.926	0.025	13.664	−0.024
1.000	1.588	0.966	0.016	13.292	−0.022
1.500	1.520	1.051	−0.004	13.798	−0.014
2.000	1.555	1.094	−0.012	13.096	−0.012
3.000	1.534	1.032	0.012	13.202	−0.039
4.000	1.505	0.992	0.030	13.634	−0.055
5.000	1.503	0.950	0.046	13.646	−0.062
6.000	1.481	0.932	0.059	13.911	−0.084
8.000	1.530	0.883	0.078	14.152	−0.098
10.000	1.503	1.014	0.051	14.188	−0.073
15.000	1.581	1.154	0.031	14.059	−0.059

$40PbO.10BaO.50B_2O_3$; $40Bi_2O_3.10BaO.50P_2O_5$; $50Bi_2O_3.30B_2O_3.5TeO_2.15SiO_2$ and $50Bi_2O_3.50B_2O_3$glasses for gamma ray shielding up to 3 MeV. Beyond 3 MeV, present glasses are better shields to above glasses. Further, HVL of the present glasses is nearly same as HVL of 50PbO.50B2O3up to 800 keV; beyond 800 keV; HVL of present glasses is lower than the HVL of $50PbO.50B_2O_3$. The HVL of the present glasses are nearly same as of $40PbO.10Bi_2O_3.49.5B_2O_3.0.5FeO$ for energies from 300 keV to 15 MeV; HVL of the present samples are lower than the HVL of

Table 6
Exposure G-P fitting parameters of WTP3 glass sample.

Energy (MeV)	WTP3				
	b	c	A	X_k	D
0.015	1.000856	2.074243	−0.31961	11.12351	0.258397
0.020	2.117564	1.481718	0.233007	12.58581	−0.3096
0.030	1.430888	0.473867	0.213462	15.15609	−0.07712
0.040	3.847722	0.550493	0.090287	24.11978	−0.05576
0.050	3.33359	0.307151	0.037709	14.8357	−0.11829
0.060	2.861953	0.19843	0.14691	6.936223	−0.06996
0.080	1.878639	0.074395	0.535801	15.72373	−0.13291
0.100	1.502637	0.083848	0.51269	15.54124	−0.11596
0.150	1.19437	0.227957	0.371354	14.30301	−0.18945
0.200	1.169416	0.407154	0.218881	14.18595	−0.11662
0.300	1.296487	0.574474	0.132842	13.83539	−0.06285
0.400	1.366679	0.690157	0.09323	14.17711	−0.05201
0.500	1.418486	0.759369	0.071832	14.13698	−0.04345
0.600	1.452502	0.80742	0.056059	13.75685	−0.03527
0.800	1.58221	0.929622	0.024059	13.66212	−0.02372
1.000	1.589994	0.966796	0.015441	13.28482	−0.0222
1.500	1.522573	1.05442	−0.00469	13.77275	−0.01324
2.000	1.538291	1.043484	0.001742	13.63226	−0.02165
3.000	1.532335	1.03513	0.011001	13.1767	−0.03851
4.000	1.496119	1.002967	0.026349	13.58277	−0.05279
5.000	1.539188	0.928951	0.055756	13.79976	−0.07957
6.000	1.483489	0.930007	0.058501	13.89506	−0.08305
8.000	1.525411	0.910602	0.067891	14.15931	−0.09831
10.000	1.502976	0.998175	0.053633	14.19536	−0.07479
15.000	1.575665	1.130485	0.033737	14.12493	−0.05944

$40PbO.10Bi_2O_3.49.5B_2O_3.0.5FeO$ glasses. Beyond 15 MeV, HVL of $40PbO.10Bi_2O_3.49.5B_2O_3.0.5FeO$ glasses is higher than the HVL of the WTP1 and WTP2 but lower than the WTP3, WTP4 and WTP5.

The Z_{eq} of the present glasses have been calculated in the energy range of 0.015–15 MeV and are represented in Table 3. The Z_{eq} ranges from 28.42 to 61.95. The variation of Z_{eq} with energy is shown in Fig. 6. The Z_{eq} rises sharply up to 0.1 MeV. Thereafter, it shows a slightly increasing trend up to 1.5 MeV. From 1.5MeV-15MeV, it shows a decreasing trend. The Z_{eq} of WTP5 glass is maximum for all energies except the energy range 0.04–0.08 MeV. It is due to the presence of higher concentration of PbO present in it. In the energy range 0.04–0.08 MeV, the Z_{eq} of all the glass samples is nearly same. It is due to the dominance of Compton scattering in the above energy region as explained earlier.

The exposure geometrical progression fitting parameters are presented in Tables 4–8 respectively. These parameters are calculated to obtain the EBF for the present glass samples in the energy range of 0.015–15 MeV. The variation of EBF with energy has been presented in Fig. 7 for penetration depths of 1, 5, 10, 20 and 40 mfp for the present glass samples. The EBF is small and nearly same for all penetration depths at 0.015 MeV. Then, it shows a sharp peak at 0.02 MeV, 0.03 MeV and 0.04 MeV. But the peaks at 0.03 MeV and 0.04 MeV are relatively very weak. These peaks are due to K-absorption edge of tellurite (Te) which lies at 0.0318 MeV and is present in highest percentage in the present glasses. From 0.04MeV to 0.2 MeV, the EBF is nearly same for all penetration depths for all the samples. Beyond 0.2 MeV, the EBF shows an increasing trend with the increase in penetration depth. It is due to the fact that EBF, which is due to the multiple scattering and the chances of multiple scattering increases with increase in penetration depth. Thus, results in an increase of EBF for higher penetration depth values.

The EBF of the present glasses has been compared with soda lime silica glass (G6) [43], lead borate glass (S7) [44], bismuth borosilicate glass (BS) [45], lead (Pb) [46], OC, IL, SC and SM [47], at penetration depths of 1, 5, 10, 20 and 40 mfp for photon energies of 0.05, 0.15, 1.5 and 15 MeV. These results are presented in Tables 9 and 10 respectively. The glasses and the concretes show similar

Table 7
Exposure G-P fitting parameters of WTP4 glass sample.

Energy (MeV)	WTP4				
	b	c	A	X_k	D
0.015	1.000241	2.166258	−0.24824	12.55483	0.226461
0.020	1.396838	0.585353	0.578229	11.41177	−0.79831
0.030	2.822042	0.862775	0.242113	25.84178	−0.16557
0.040	3.856483	0.529032	0.090073	24.04936	−0.05354
0.050	3.320237	0.291149	0.01662	14.66473	−0.10794
0.060	2.834584	0.186708	0.204552	7.57432	−0.07466
0.080	1.871984	0.068987	0.561728	15.69794	−0.14074
0.100	1.480054	0.052815	0.615314	14.79307	−0.15086
0.150	1.197761	0.154201	0.466304	19.46592	−0.03679
0.200	1.178619	0.423193	0.209942	14.19121	−0.11205
0.300	1.304299	0.578224	0.131592	13.83852	−0.06248
0.400	1.376214	0.694573	0.092026	14.16607	−0.05171
0.500	1.425606	0.763838	0.07062	14.13319	−0.04309
0.600	1.46029	0.812923	0.05462	13.76193	−0.03481
0.800	1.506768	0.87258	0.03786	13.68972	−0.02786
1.000	1.597186	0.971111	0.014578	13.25797	−0.0222
1.500	1.524194	1.056268	−0.00515	13.7588	−0.01298
2.000	1.543619	1.043671	0.001835	13.69302	−0.02196
3.000	1.530239	1.040265	0.009429	13.13478	−0.0373
4.000	1.487727	1.013259	0.023024	13.53369	−0.05025
5.000	1.52049	0.939613	0.052048	13.75803	−0.07703
6.000	1.569408	0.907094	0.067988	14.06275	−0.08827
8.000	1.526785	0.902585	0.070868	14.15702	−0.09836
10.000	1.502531	0.983057	0.056079	14.20203	−0.07643
15.000	1.590024	1.197743	0.026936	13.936	−0.05694

Table 8
Exposure G-P fitting parameters of WTP5 glass sample.

Energy (MeV)	WTP5				
	b	c	A	X_k	D
0.015	1.005706	1.056927	0.003534	12.01472	0.039838
0.020	2.208609	1.594951	0.189397	12.73411	−0.24786
0.030	1.555723	0.508765	0.216033	16.11497	−0.08506
0.040	3.872419	0.489997	0.089682	23.92127	−0.0495
0.050	3.300659	0.267686	−0.0143	14.41405	−0.09276
0.060	2.808674	0.175611	0.259123	8.178406	−0.07911
0.080	1.867695	0.065502	0.578437	15.68132	−0.14578
0.100	1.600427	0.218226	0.068312	18.78094	0.035185
0.150	1.197251	0.165297	0.45202	18.68921	−0.05975
0.200	1.183586	0.43185	0.205116	14.19405	−0.10958
0.300	1.239605	0.54717	0.141943	13.81264	−0.06558
0.400	1.389836	0.700882	0.090305	14.15029	−0.0513
0.500	1.439472	0.772541	0.06826	14.12581	−0.04238
0.600	1.471221	0.820645	0.052601	13.76906	−0.03415
0.800	1.517189	0.88046	0.035953	13.68591	−0.02729
1.000	1.530951	0.931371	0.022526	13.50525	−0.0222
1.500	1.530025	1.062912	−0.00677	13.70862	−0.01206
2.000	1.549219	1.043867	0.001934	13.75688	−0.02228
3.000	1.527534	1.046891	0.007401	13.08068	−0.03573
4.000	1.485057	1.016534	0.021966	13.51807	−0.04945
5.000	1.498997	0.95187	0.047784	13.71008	−0.07412
6.000	1.540305	0.915433	0.065095	14.0168	−0.08696
8.000	1.687806	0.92109	0.074483	14.17011	−0.09441
10.000	1.530707	1.037129	0.047161	14.17226	−0.07017
15.000	1.585271	1.175481	0.029187	13.99854	−0.05777

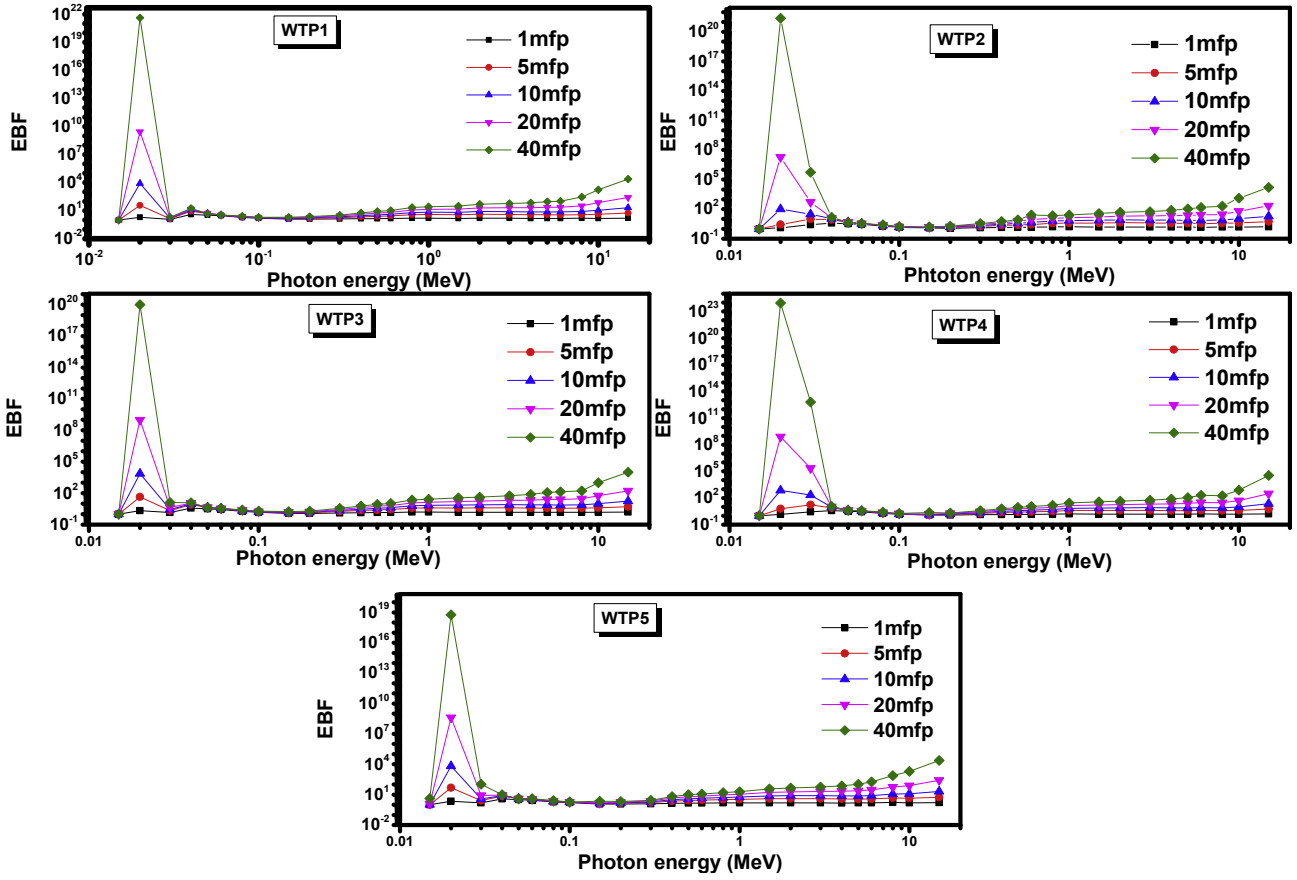

Fig. 7. Variation of EBF of $20WO_3$-(80-x)TeO_2-xPbO glasses with photon energy at 1, 5, 10, 20 and 40 mfp.

Table 9
Comparison of EBF of $20WO_3$-(80-x)TeO_2-xPbO glasses with G6, S7, BS glasses and lead at penetration depths 1, 5, 10, 20 and 40 for photon energies 0.05, 0.15, 1.5 and 15 MeV.

Energy (MeV)	WTP1	WTP2	WTP3	WTP4	WTP5	G6	S7	BS	Lead
(a) EBF for 1 mfp									
0.05	3.37	3.35	3.33	3.32	3.30	1.17	1.02	1.13	1.02
0.15	1.21	1.19	1.19	1.20	1.20	1.84	1.39	1.24	1.40
1.50	1.50	1.52	1.52	1.52	1.53	1.78	1.74	1.60	1.38
15.00	1.59	1.58	1.58	1.59	1.59	1.24	1.25	1.22	1.63
(b) EBF for 5 mfp									
0.05	4.88	4.62	4.44	4.29	4.11	1.28	1.04	1.27	1.04
0.15	1.40	1.32	1.33	1.29	1.30	4.49	2.16	1.57	1.84
1.50	3.64	3.84	3.87	3.88	3.94	6.05	5.72	4.66	2.74
15.00	5.64	5.43	5.22	5.84	5.63	2.09	2.09	2.08	6.83
(c) EBF for 10 mfp									
0.05	5.06	4.70	4.48	4.30	4.09	1.32	1.06	1.34	1.05
0.15	1.51	1.40	1.41	1.36	1.37	7.53	2.76	1.79	2.13
1.50	6.71	7.27	7.34	7.38	7.54	13.21	12.33	9.64	4.47
15.00	20.96	19.13	17.39	22.81	20.86	3.32	3.16	3.45	30.87
(d) EBF for 20 mfp									
0.05	5.11	4.68	4.43	4.24	4.01	1.35	1.07	1.45	1.06
0.15	1.71	1.52	1.56	1.52	1.54	14.09	3.78	2.16	2.87
1.50	14.22	15.80	16.02	16.14	16.57	31.56	29.22	22.62	8.11
15.00	259.00	211.35	170.42	311.94	256.23	7.07	5.85	8.35	1.07E+03
(e) EBF for 40 mfp									
0.05	4.75	4.36	4.15	3.98	3.80	1.37	1.09	1.53	1.08
0.15	1.92	1.60	1.75	2.25	2.25	27.34	5.20	2.62	6.65
1.50	31.04	35.59	36.20	36.54	37.78	79.37	72.39	55.48	15.00
15.00	2.40E+04	1.57E+04	1.00E+04	3.52E+04	2.35E+04	22.16	12.11	30.88	5.59E+05

Table 10
Comparison of EBF of 20WO3-(80-X)TeO2-XPbO glasses with different types of concretes at penetration depths 1, 5, 10, 20 and 40 for photon energies 0.05, 0.15, 1.5 and 15 MeV.

Energy (MeV)	WTP1	WTP2	WTP3	WTP4	WTP5	OC	IL	SC	SM
(a) EBF for 1 mfp									
0.05	3.37	3.35	3.33	3.32	3.30	1.04	1.01	1.01	1.01
0.15	1.21	1.19	1.19	1.20	1.20	2.91	1.99	1.87	1.79
1.50	1.50	1.52	1.52	1.52	1.53	1.91	1.80	1.78	1.76
15.00	1.59	1.58	1.58	1.59	1.59	1.26	1.24	1.22	1.21
(b) EBF for 5 mfp									
0.05	4.88	4.62	4.44	4.29	4.11	1.09	1.02	1.03	1.03
0.15	1.40	1.32	1.33	1.29	1.30	16.68	5.59	1.96	4.19
1.50	3.64	3.84	3.87	3.88	3.94	7.19	6.17	6.07	5.87
15.00	5.64	5.43	5.22	5.84	5.63	2.09	2.09	2.08	2.06
(c) EBF for 10 mfp									
0.05	5.06	4.70	4.48	4.30	4.09	1.11	1.03	1.03	1.03
0.15	1.51	1.40	1.41	1.36	1.37	50.10	10.23	1.96	6.83
1.50	6.71	7.27	7.34	7.38	7.54	16.42	13.46	13.37	12.75
15.00	20.96	19.13	17.39	22.81	20.86	3.09	3.33	3.45	3.52
(d) EBF for 20 mfp									
0.05	5.11	4.68	4.43	4.24	4.01	1.14	1.02	1.02	1.02
0.15	1.71	1.52	1.56	1.52	1.54	193.53	21.19	1.96	12.34
1.50	14.22	15.80	16.02	16.14	16.57	40.34	31.89	32.65	30.45
15.00	259.00	211.35	170.42	311.94	256.23	5.51	7.26	8.26	9.27
(e) EBF for 40 mfp									
0.05	4.75	4.36	4.15	3.98	3.80	1.16	1.02	1.02	1.02
0.15	1.92	1.60	1.75	2.25	2.25	940.68	46.10	1.94	22.89
1.50	31.04	35.59	36.20	36.54	37.78	105.85	77.84	85.17	76.26
15.00	2.40E+04	1.57E+04	1.00E+04	3.52E+04	2.35E+04	10.59	21.35	29.70	42.09

behavior when EBF of the present glasses are compared with them except for lead. It is found that the glasses and the standard shielding concretes possess lower values of EBF at low and very high energies at all penetration depths. Whereas possesses higher values of EBF in the medium energy range for all penetration depths. It is also found that the gap in the values shows increasing with increase in penetration depth at higher energies. In case of Pb, the EBF of all the present glasses are higher at 0.05 MeV, lower at 0.15 MeV, higher at 1.5 MeV and lower at 15 MeV than EBF of Pb. Similar observations are observed for all penetration depths when EBF of the present glasses and Pb are compared.

4. Conclusion

From the obtained results we can conclude that the μ/ρ, MFP, HVL and EBF vary with energy and chemical composition of the glass. The penetration depth is also found to affect the EBF. Besides, the addition of PbO into the glass system increases enhances the shielding properties of the present glass system. It has been found that the present glasses have higher μ/ρ when compared to commercial window glasses. When compared with different glasses and some standard shielding concretes, most of the present glasses have lower values of MFP and HVL than the other glasses and concretes, thus indicating the availability of utilizing the WO_3-

TeO_2-PbOglass systemas substitutes for some commercial window glasses and concretes with respect to gamma rayprotection. WTP5 is the best sample for radiation shielding as it contains a higher percentage of PbO.

References

[1] I. Akkurt, C. Basyigit, S. Kilincarslan, B. Mavi, A. Akkurt, Radiation shielding of concretes containing different aggregates, Cement Concr. Compos. 28 (2006) 153–157.
[2] Chang-Min Lee, Yoon Hee Lee, Kun Jai Lee, Cracking effect on gamma-ray shielding performance in concrete structure, Prog. Nucl. Energy 49 (2007) 303–312.
[3] B.O. El-bashir, M.I. Sayyed, M.H.M. Zaid, K.A. Matori, Comprehensive study on physical, elastic and shielding properties of ternary BaO-Bi2O3-P2O5 glasses as a potent radiation shielding material, J. Non-Cryst. Solids 468 (2017) 92–99.
[4] Narveer Singh, Kanwar Jit Singh, Kulwant Singh, Harvinder Singh, Comparative study of lead borate and bismuth lead borate glass systems as gamma-radiation shielding materials, Nucl. Instrum. Meth. Phys. Res. B 225 (2004) 305–309.
[5] M.I. Sayyed, G. Lakshminarayana, Structural, thermal, optical features and shielding parameters investigations of optical glasses for gamma radiation shielding and defense applications, J. Non-Cryst. Solids 487 (2018) 53–59.
[6] M.I. Sayyed, Half value layer, mean free path and exposure buildup factor for tellurite glasses with different oxide compositions, J. Alloy. Comp. 695 (2017) 3191–3197.
[7] M.I. Sayyed, H. Elhouichet, Variation of energy absorption and exposure buildup factors with incident photon energy and penetration depth for boro-tellurite (B_2O_3-TeO_2) glasses, Radiat. Phys. Chem. 130 (2017) 335–342.
[8] R. El-Mallawany, H. Afifi, Elastic moduli and crosslinking of some tellurite glass systems, Mater. Chem. Phys. 143 (2013) 11–14.
[9] G. Lakshminarayana, S.O. Baki, A. Lira, M.I. Sayyed, I.V. Kityk, M.K. Halimah, M.A. Mahdi, X-ray photoelectron spectroscopy (XPS) and radiation shielding parameters investigations for zinc molybdenum borotellurite glasses containing different network modifiers, J. Mater. Sci. 52 (2017) 7394–7414.
[10] Hong-Wei Li, Shi-Qing Man, Optical properties of Er^{3+} in MoO_3–Bi_2O_3–TeO_2 glasses, Optic Commun. 282 (2009) 1579–1583.
[11] O.A. Zamyatin, A.D. Plekhovich, E.V. Zamyatina, A.A. Sibirkin, Glass-forming region and physical properties of the glasses in the TeO_2 – MoO_3 – Bi_2O_3 system, J. Non-Crystall. Solids 452 (2016) 130–135.
[12] P.S.R. Naik, M.K. Kumar, Y.N. Ch, R. Babu, A.S. Kumar, Spectroscopic studies of Eu^{3+}:PbO–Bi_2O_3–WO_3–B_2O_3 glasses, Indian J Phys 87 (8) (2013) 757–762.
[13] M. Milanova a, R. Iordanova, K.L. Kostov, Glass formation and structure of glasses in the MoO_3–CuO–Bi_2O_3 system, Phys. Chem. Glasses: Eur. J. Glass Sci. Technol. B 48 (4) (2007) 255–258.
[14] Gopi Sharma, Kulwant Singh, Manupriya, Shaweta Mohan, Harvinder Singh, Sukhleen Bindra, Effects of gamma irradiation on optical and structural properties of PbO–Bi2O3–B2O3 glasses, Radiat. Phys. Chem. 75 (2006) 959–966.
[15] M.I. Sayyed, M.Y. AlZaatreh, M.G. Dong, M.H.M. Zaid, K.A. Matori, H.O. Tekin, A comprehensive study of the energy absorption and exposure buildup factors of different bricks for gamma-rays shielding, Results Phys. 7 (2017) 2528–2533.
[16] Huseyin Ozan Tekin, M.I. Sayyed, Tugba Manici, Elif Ebru Altunsoy. Photon shielding characterizations of bismuth modified borate silicate tellurite glasses using MCNPX Monte Carlo code, Mater. Chem. Phys. 211 (2018) 9–16.
[17] R. El-Mallawany, M.I. Sayyed, M.G. Dong, Comparative shielding properties of some tellurite glasses: Part 2, J. Non-Cryst. Solids 474 (2017) 16–23.
[18] S. Singh, D. Ashok Kumar, K.S. Singh, G. Thind, S. Mudahar, Barium–borate–flyash glasses: as radiation shielding materials, Nucl. Instrum. Methods Phys. Res. B 266 (2008) 140–146.
[19] Ashok Kumar, Gamma ray shielding properties of PbO-Li_2O-B_2O_3 glasses, Radiat. Phys. Chem. 136 (2017) 50–53.
[20] I. Akkurt, H. Akyıldırıma, B. Mavi, S. Kilincarslan, C. Basyigit, Radiation shielding of concrete containing zeolite, Radiat. Meas. 45 (2010) 827–830.
[21] I.I. Bashter, Calculation of radiation attenuation coefficients for shielding concretes, Ann. Nucl. Energy 24 (1997) 1389–1401.
[22] B. Oto, N. Yildiz, T. Korkut, E. Kavaz, Neutron shielding qualities and gamma ray buildup factors of concretes containing limonite ore, Nucl. Eng. Des. 293 (2015) 166–175.
[23] S.S. Obaid, D.K. Gaikwad, P.P. Pawar, Determination of gamma ray shielding parameters of rocks and concrete, Radiat. Phys. Chem. 144 (2017) 356–360.
[24] S. Shamsan, M.I. Obaid, D.K. Sayyed, Gaikwad, P. Pravina, Pawar, Attenuation coefficients and exposure buildup factor of some rocks for gamma ray shielding applications, Rad. Phys. Chem. 148 (2018) 86–94.
[25] I. Han, L. Demir, Mass attenuation coefficients, effective atomic and electron numbers of Ti and Ni alloys, Radiat. Meas. 44 (2009) 289–294.
[26] Iskender Akkurt, Effective atomic and electron numbers of some steels at different energies, Ann. Nucl. Energy 36 (2009) 1702–1705.
[27] D.K. Gaikwad, P.P. Pawar, T.P. Selvam, Measurement of attenuation cross-sections of some fatty acids in the energy range 122–1330 keV, Pramana-J. Phys. 87 (12) (2016) 1–7.
[28] D.K. Gaikwad, P.P. Pawar, T.P. Selvam, Mass attenuation coefficients and effective atomic numbers of biological compounds for gamma ray interactions, Radiat. Phys. Chem. 138 (2017) 75–80.
[29] V.V. Awasarmol, D.K. Gaikwad, S.D. Raut, P.P. Pawar, Gamma ray interaction studies of organic nonlinear optical materials in the energy range 122 keV-1330 keV, Results Phys. 130 (2017) 343–350.
[30] S.R. Manohara, S.M. Hanagodimath, L. Greward, Studies on effective atomic number, electron density and kerma for some fatty acids and carbohydrates, Phys. Med. Biol. 53 (2008) N377–N386.
[31] R.R. Bhosale, D.K. Gaikwad, P.P. Pawar, M.N. Rode, Effects of gamma irradiation on some chemicals using an NaI (Tl) detector, Radiat. Eff. Defect Solid 171 (2016) 398–407.
[32] A. Un, Y. Yahin, Determination of mass attenuation coefficients, effective atomic and electron numbers, mean free paths and kermas for PbO, barite and some boron ores, Nucl. Instrum. Meth. Phys. Res. B 269 (2011) 1506–1511.
[33] V.P. Singh, N.M. Badiger, J. Kaewkhao, Radiation shielding competence of some silicate and borate heavy metal oxide glass systems: Comparative study, J. Non-Cryst. Solids 404 (2014) 167–173.
[34] S. Singh, S.S. Ghumman, C. Singh, K. Singh Thind, G.S. Mudahar, Buildup of gamma ray photons in flyash concretes: a study, Ann. Nucl. Energy 37 (2010) 681–684.
[35] M.I. Sayyed, Bismuth modified shielding properties of zinc boro-tellurite glasses, J. Alloy. Comp. 688 (2016) 111–117.
[36] A.M.A. Mostafa, Shams A.M. Issa, M.I. Sayyed, Gamma ray shielding properties of PbO-B2O3-P2O5 doped with WO3, J. Alloy. Comp. 708 (2017) 294–300.
[37] Hesham Afifi, Samier Marzouk, Ultrasonic velocity and elastic moduli of heavy metal tellurite glasses, Mater. Chem. Phys. 80 (2003) 517–523.
[38] P. Fuochi, U. Corda, M. Lavalle, A. Kovacs, M. Baranyai, A. Mejri, K. Arah, Dosimetric properties of gamma and electron-irradiated commercial window glasses, Nukleonika 54 (2009) 39–43.
[39] Adem Un, Faruk Demir, Deteramination of mass attenuation coefficents, effective atomic numbers and effective electron numbers for heavy-weight and normal-weight concretes, Appl. Radiat. Isot. 80 (2013) 73–77.
[40] Narveer Singh, Kanwar Jit Singh, Kulwant Singh, Harvinder Singh, Gamma-ray attenuation studies of PbO-BaO-B2O3 glass system, Radiat. Meas. 41 (2006) 84–88.
[41] Shams A.M. Issa, A.M.A. Mostafa, Effect of Bi2O3 in borate –tellurite-silicate glass system for development of gamma-rays shielding materials, J. Alloy. Comp. 695 (2017) 302–310.
[42] S. Atul Khanna, S. Bhatti, K.J. Singh, K.S. Thind, Gamma-ray attenuation coefficents in some heavy metal oxide borae glasses at 662 keV, Nucl. Instrum. Meth. Phys. Res. B 114 (1996) 217–220.
[43] M.I. Sayyed, Y. Elmahroug, B.O. Elbashir, Shams A.M. Issa, Gamma-ray shielding properties of zinc oxide soda lime silica glasses, J Mater Sci: Mater. Electron. 28 (2017) 4064–4074.
[44] V.P. Singh, N.M. Badiger, Shielding efficiency of lead borate and nickel borate glasses for gamma rays and neutrons, Glass Phys. Chem. 41 (2015) 276–283.
[45] VishwanathP. Singh, N.M. Badiger, N. Chanthima, J. Kaewkhao, Evaluation of gamma-ray exposure buildup factors and neutron shielding for bismuth borosilicate glasses, Rad. Phys. Chem. 98 (2014) 14–21.
[46] ANSI/ANS-6.4.3, Gamma ray attenuation coefficient and buildup factors for engineering materials, American nuclear Society, La Grange Park, 1991.
[47] Updesh Kaur, J.K. Sharma, Parjit S. Singh, TejbirSingh, Comparative studies of different concretes on the basis of some photon interaction parameters, Appl. Radiat. Isot. 70 (2012) 233–240.
[48] A.E. Ersundua, M. Büyükyıldızb, M. Çelikbilek Ersundua, E. Şakarc, M. Kurudirekc, The heavy metal oxide glasses within the WO3-MoO3-TeO2 system to investigate the shielding properties of radiation applications, Prog. Nucl. Energy 104 (2018) 280–287.
[49] J.H. Hubbell, S.M. Seltzer, Tables of X-Ray Mass Attenuation Coefficients and Mass Energy-Absorption Coefficients 1 Kev–20 Mev for Elements $1 \leq Z \leq 92$ and 48 Additional Substances of Dosimetric Interest, National Institute of Standarts and Physics Laboratory, NISTIR, 1995, p. 5632.
[50] M.J. Berger, J.H. Hubbell, (XCOM) Photon Cross Section on a Personal Computer NBSIR.87, 3597, NIST, 1987.
[51] Y. Harima, An approximation of gamma buildup factors by modified geometrical progression, Nucl.Sci.Eng. 83 (1983) 299–309.
[52] M.I. Sayyed, I. Saleem, Z.Y. Qashou, Khattari, Radiation shielding competence of newly developed TeO2-WO3 glasses, J. Alloy. Comp. 696 (2017) 632–638.
[53] Mengge Dong, Xiangxin Xue, Ashok Kumar, He Yang, M.I. Sayyed, Shan Liu, Erjun Bu, A novel method of utilization of hot dip galvanizing slag using the heat waste from itself for protection from radiation, J. Hazard Mater. 344 (2018) 602–614.